

SYNTHESIS OF α - ALUMINA FROM A LESS COMMON RAW MATERIAL

Aurora López-Delgado^{a*}, Laila Fillali^{a,b}, Jose A. Jiménez^a and Sol López-Andrés^b

^a National Centre for Metallurgical Research, CSIC. Avda, Gregorio del Amo, 8. 28040 Madrid. Spain.

^b Dpt. Crystallography and Mineralogy. Faculty of Geology, UCM. 28040 Madrid. Spain.

*Corresponding author: Tel.: +34915538900, fax: +34915347425.

E-mail address: alopezdelgado@cenim.csic.es

Abstract

A nanostructured α -Al₂O₃ with particle size lower than 100 nm was obtained from a hazardous waste generated in slag milling process by the aluminium industry. The route developed to synthesize alumina consisted of two steps: in the first one, a precursor of alumina, boehmite, γ -AlOOH was obtained by a sol-gel method. In the second step, the alumina was obtained by calcination of the precursor boehmite (xerogel). Calcination in air was performed at two different temperatures, i.e 1300 and 1400 °C, to determine the influence of this parameter on the quality of resulting alumina. X-ray diffraction patterns and transmission electron microscopy images of calcined powders revealed beside corundum the presence of transition aluminas and some rest of amorphous phase in the sample prepared at 1300 °C. The increase of the calcinations temperature to 1400 °C favors the formation of an almost single-phase corundum powder. The transition of θ - to α -Al₂O₃ was followed by means of Infrared spectroscopy, since it is accompanied by the disappearance of the IR band frequencies associated with tetrahedral sites (AlO₄ sites), giving rise to a spectrum dominated by Al³⁺ ions in octahedral sites (AlO₆) characteristic of corundum.

Keywords: alpha-alumina · boehmite · sol-gel · non-conventional raw material.

1. Introduction

Polymorphic crystalline aluminium oxides with the chemical formula Al_2O_3 , and commonly referred with the generic name of alumina, are extensively used in numerous industrial applications (ceramics, abrasive materials, absorbents, catalysts, biomaterials, composites, pigments, etc) [1-4]. Among the various structural forms, only the alpha alumina ($\alpha\text{-Al}_2\text{O}_3$), or corundum is the thermodynamically stable. Commercial aluminas are mainly prepared by thermal decomposition of precursors, which are generally produced by precipitation of aluminium oxy-hydroxides from solution of reagent grade aluminium salts [5,6]. Depending on the condition of the synthesis, they are formed in different modifications that differ in chemical composition and crystal structure. Boehmite is one of the most popular precursors of alumina, and its transformation into $\alpha\text{-Al}_2\text{O}_3$ involves a complex transformation sequence of transitional aluminas [3,7,8]. However, the transition sequences depend strongly on the chemical routes in synthesis, atmospheric conditions, degree of crystallinity, heating rates, impurities, moisture, alkalinity, the thermal history of the material, etc. [8-10]. Sol-gel process and Pechini's method are widely used for the preparation of alumina precursor [11,12]. But, new methods such as spray pyrolysis technique [13], or improved ones such as sol-gel polymeric method [10,14] allows to prepare nano-sized materials, which show superior homogeneity and microstructures leading to unique physical properties [15].

The environmental policies of industrialized countries seek nowadays to save natural resources through the use of secondary resources. In Europe, this strategy is promoted by the Directive of the European Parliament and of the Council on Waste (European Directive 2008/98/EC). Thus a number of researches have been focused on the use of waste for different applications and uses [16]. In this work, a less common raw material such as a hazardous waste obtained by the tertiary aluminium industry in the milling slag process was used as aluminous source for the synthesis of fine $\alpha\text{-Al}_2\text{O}_3$ particle powders. From a mineralogical point of view, the waste consisted principally of corundum, spinel, metallic aluminium, quartz, aluminium nitride, calcite, iron oxide, aluminium sulfide and other minor oxides and salts. The total aluminium content ranges from 25 to 40 % (wt). This waste is a heterogeneous material from the physical-chemical point of view because it is strongly dependant on the type and quality of the processed scrap, the classification and trapping methods used, etc. It is considered as hazardous in the European legislation due to the release of toxic gases (hydrogen, ammonia, hydrogen sulfide, etc) in the presence of humidity [17].

The aim of this work is to recover the aluminium content of the hazardous waste as a highly valuable product, $\alpha\text{-Al}_2\text{O}_3$ (corundum). For this goal, a new processing route was developed, that includes the hydrothermal treatment of the waste to recover the aluminium content and the subsequent obtaining of the alumina precursor, boehmite, ($\gamma\text{-AlOOH}$) by sol-gel. In the second step, the alumina was obtained by calcination of the boehmite xerogel. The thermal transformation of boehmite into alumina was followed by simultaneous thermogravimetric/differential thermal analysis (TG/DTA). Finally, calcination in air was performed at two different temperatures, i.e. 1300 and 1400 °C, to determine the influence of this parameter on the quality of resulting alumina. The resulting materials were characterized by x-ray diffraction (XRD),

x-ray fluorescence (XRF) and scanning and transmission electron microscopy (SEM/TEM), and infrared spectroscopy (FTIR).

2. Materials and Methods

2.1 Materials

The waste product used in this work is a very fine grey colored powder, with a characteristic odor derived from its aluminium nitride, carbide and sulfide contents. It comes from the fine suction system used in the slag milling operation and was supplied by a tertiary aluminium industry (Recuperaciones y Reciclajes Roman S.L. Fuenlabrada, Madrid, Spain). The major mineralogical composition of the waste, expressed as wt. %, is as follows: Al^o 31.2, Al₂O₃ (corundum) 20.0, MgAl₂O₄ (spinel) 15.0, AlN 8.4, SiO₂ (quartz) 8.0, CaCO₃ (calcite) 8.2, Fe₂O₃ (hematite) 1.8, TiO₂ 1.5, chloride (Na/K) 1.5, Al₂S₃0.7 and other minor metal oxides.

2.2 Synthesis of the precursor

The process described by Gonzalo-Delgado et al. [17] was followed to obtain the precursor boehmite. Thus 50 g of the waste were heat treated and vigorously stirred with 50 mL of a solution of HCl (10% v/v) to dissolve the aluminium compounds during 150 min. The Al³⁺ solution obtained, with a pH lower than 2 was separated from the solid residue by filtration in a pressure system (Millipore YT30 142 HW with 0.2 μm Isopore membrane filters). Then, the acid solution was subjected to alkalization by dropwise adding a 1 N NaOH solution up to pH 8. The colloidal suspension (sol) starts to appear at low pH values and massive gelification takes place around pH 6. The gelled emulsion was kept stirring for 24 h. Gel was converted to xerogel by drying at 150 °C for 24 h, and then crushed in a mortar to get a fine powder.

2.3 Characterization of precursor and calcined products

The thermal transformation of the precursor boehmite into alumina was followed by simultaneous thermogravimetry/differential thermal analysis (TG/DTA) in a Seteram DTA-TG Setsys Evolution 500 at a heating rate of 20 °Cmin⁻¹, in air up to 1400 °C. Alumina crucibles with 20mg samples were used. Calcinations of the precursor were carried out at 1300 and 1400 °C in a high alumina refractory crucible using an electrical muffle furnace (Thermoconcept HT0417). The temperature was raised to the selected calcinations temperature at the same heating rate used for the TG/DTA analysis.

The chemical composition of samples was determined by X-ray fluorescence (XRF, Panalytical Axios wavelength-dispersive X-ray spectrometer) on 37 mm disk diameter of compacted samples. X-ray

diffraction measurements for identification of crystalline phases were carried out in a Bruker D8 advance diffractometer equipped with $\text{Cu}_{K\alpha}$ tube. A current of 30 mA and a voltage of 40 kV were employed as tube setting. XRD data were collected over a 2θ range of 10-100 ° with a step width of 0.02 ° and a counting time of 10 s/step.

The morphological characterization of the samples was performed by Field Emission Gun Scanning Electron Microscopy scanning electron microscopy (Jeol JSM-6500F). For those observations, the powdered sample was embedded in a polymeric resin and sputter coated with graphite to make the sample conductive. A Jeol FEM-2100 transmission electron microscope operated at 200 KeV was used for the characterization of calcined samples and to study the structure on the atomic level. For TEM observations samples were prepared by ultrasonic dispersion of powder in acetone and the suspension was placed on a 3 mm carbon coated copper grid. High resolution imaging HRTEM was performed to analyze the crystalline quality of calcined powders. Selected-area electron diffraction (SAED) has been also used for elucidating the presence of amorphous phase and crystalline structure in some regions of the aggregates observed in the calcined powders.

Fourier-Transform infrared (FTIR) spectra were recorded on sample/CsI discs, in the 1400-200 cm^{-1} range using a Nicolet Magna-IR 550 spectrophotometer (CsI beam splitter).

3. Results and discussion

3.1 Characterization of the waste and the precursor

The XRD pattern of the aluminium waste is shown in Fig. 1. The crystalline phases identified by comparison with the powder diffraction data (JCPDS files) are metallic aluminium (1), corundum (2), silica (3), aluminium nitride (4), calcium carbonate (5) and spinel (6). Besides, a certain amount of amorphous phases is inferred from the background. Compared with the XRD analysis report by Gonzalo-Delgado et al. [17], some minor differences were found, which can be attributed to the heterogeneity of the waste.

As shown in Fig. 2, the XRD pattern of the precursor (xerogel), obtained by the hydrothermal treatment of the waste, consists of 6 broad boehmite diffraction peaks, indicating a very small grain and relatively low crystallinity. In this figure, reflections were indexed according to JCPDS file 1-088-2112. The chemical analysis of this precursor boehmite obtained by XRF and expressed as oxides wt.%, was Al_2O_3 61.53, Fe_2O_3 2.05, SiO_2 0.64, ZnO 0.33, CuO 0.11, Cr_2O_3 0.09, PbO 0.03. The balanced water was 31.8 wt. %. It was also determined an amount of 3.20 wt.% chloride in the sample, which comes from the first stage in the synthesis process. Taking into account the aluminium content in the waste, the 90 wt.% was recovered as boehmite of relatively high purity.

Fig. 3 shows FEG-SEM micrographs of precursor boehmite which consists of small (size below 100 nm) smooth round particles with certain level of agglomeration. The size grain and the low agglomeration level indicate a certain degree of crystallinity as seen in XRD pattern of Fig. 2.

3.2. Thermal study of the precursor

The result of TG/DTA studies are summarized in Table 1. The dehydration and dehydroxylation of the precursor boehmite takes place through an almost continuous mass loss up to 1028 °C. Two clear, although overlapped endothermic effects centered at 123 and 404 °C are associated to the elimination of water and the decomposition of boehmite [7,18]. The respective mass losses in these reactions are 12.7 and 15.1 wt.%. Besides, an additional small mass loss of 2.6 wt.% occurs between 500 and 1028 °C, which corresponds to a not well-defined zone in DTA curve. The total mass loss observed for the precursor by TG fits well with the value obtained by FRX analysis and lets establish the stoichiometry $\text{AlOOH}\cdot n\text{H}_2\text{O}$, ($n\sim 0.8$). Mass losses ranged between 18-25 wt.% are reported in literature for the transformation of boehmite into alumina (17 wt.% for non-hydrated boehmite) depending on the water contain both on the surface and in the boehmite structure [6, 19]. Dehydroxylation process of boehmite occurs through several process involving partial loss of water, and accordingly intermediate oxy-hydroxide compounds are formed prior to total dehydroxylation process [19]. The transformation of metastable aluminas takes also place in this zone, and in our case, besides the chloride elimination. Taking in account those results, the well defined exothermic peaks taking place between 1062-1204 °C without associated mass loss was associated to the transformation of metastable aluminas into corundum. Thus, the precursor boehmite was calcined at 1300 and 1400 °C for 7 h in air to ensure the complete formation of corundum.

3.3 Characterization of calcined precursor

The chemical composition of the precursor boehmite calcined a 1300 and 1400 °C 7 h in air was determined by XRF, and it is expressed as oxide wt % in Table 2. Both calcined products exhibits very similar compositions, with near 95 % of aluminium oxide. Chloride was not detected as expected according to thermal analysis above described. XRD patterns of these calcined samples correspond to a highly crystalline material with narrow and well-defined diffraction peaks, as shown in Figure 4. Diffraction peaks of both patterns were assigned to the hkl reflections reported in the JCPDS file 1-089-7717 for the $\alpha\text{-Al}_2\text{O}_3$ (corundum). A direct comparison between these two spectra shows that with increasing calcination temperature, the diffraction peak intensity (measured as area of diffraction peaks) increases and the width of all the XRD peaks decreases. A higher calcination temperature enhances atomic mobility, causes grain growth, and results in better crystallinity. The XRD pattern of the sample calcined at 1300 °C presents also several broad weak reflections, which can be attributable to metastable aluminas such as $\gamma\text{-Al}_2\text{O}_3$ and/or $\theta\text{-Al}_2\text{O}_3$. These phases are negligible in the pattern of sample obtained at 1400 °C.

Figure 5 shows a TEM image of precursor boehmite powders calcined at 1300 °C, which consists of aggregates of particles lower than 100 nm in size. These particles are mostly crystalline particles, as showed by the electron diffraction of a marked zone (image in the upper right corner of Figure 5). Selected-area electron diffraction confirmed also the presence of very small amorphous particles along with the crystalline ones, as showed in the upper left corner of Figure 5. This would indicate that crystalline corundum is under formation, that is, the complete mass of the precursor is not totally crystallized at this temperature.

Figure 6 (a) shows TEM image of precursor boehmite powders calcined at 1400 °C, which consists of aggregate of very small round plates, some of them with a certain tendency to present a hexagonal shape. Electron diffraction of these particles showed that all of them are crystalline, as in the upper left corner of Fig. 6a. In this case, selected-area electron diffraction confirmed the absence of amorphous phases. In the Fig. 6b is showed a high resolution TEM image, which was acquired in the marked zone in Fig. 6a. The distance between the crystallographic planes observed was 3.59 Å, which fits with the interplanar distance between (012) crystal planes of corundum. The crystals are pseudomorphs from the precursor boehmite in agreement to Souza et al. [2], who indicated the particle shape of the α -Al₂O₃ varies with the nature of the precursor, this means, the formation of corundum takes place through a topotactic reaction of boehmite dehydration [9,20].

FTIR spectra recorded on samples calcined at 1300 and 1400°C are presented in Fig. 7 along with the spectrum corresponding to precursor boehmite. The assignment of the principal bands of boehmite, according to the literature [3,17,21] are listed in Table 3. The bands corresponding to the stretching vibrations of O-H were not included. The skeleton vibrations appear at 364 cm⁻¹ as a sharp band with a shoulder at 329 cm⁻¹. Both position and broadness of bands are very sensitive to the crystallinity of samples. In this case, the broadness of bands at 496, 566 and 634 cm⁻¹ fit much better with the fundamental modes of vibration of amorphous or nanocrystalline than bulk crystal boehmite [21] in accordance with XRD results. Concerning sample obtained at 1300 °C, bands at 380 and 443, 584 and 638 cm⁻¹ can be attributable to bending (lowest ones) and stretching (highest ones) modes of Al-O bonds in the AlO₆ group of the rhombohedral α -Al₂O₃. Besides the broadness of the bands seems indicate the presence of transitional aluminas. Two peaks are also observed at 328 and 760 cm⁻¹ which can be respectively assigned to bending and stretching modes of AlO₄ group of θ -Al₂O₃ [3]. These bands are not observed in the FTIR of sample obtained a 1400 °C. In this sample, bands at 445 and 585 cm⁻¹ become narrower than in the samples calcined at 1300 °C, which indicates the transformation of the transitional aluminas to corundum. According to Boumaza et al. [3], in this transition the tetrahedral sites (AlO₄) of the phase θ disappear with temperature to give rise the characteristic octahedral sites (AlO₆) of α -Al₂O₃. IR spectroscopy results are therefore coherent with the evolution of the phases present observed by XRD.

4. Conclusions

The process developed in this work allows to obtaining a finely divided powder of nano-sized particles of corundum from a less common raw material as a hazardous waste from aluminium industry. The process involves the preparation of a xerogel of boehmite as a precursor which is transformed into alumina by calcinations. Calcination at 1300 °C determines the presence of some amount of metastable alumina and amorphous phase. A higher calcination temperature enhances atomic mobility, causes grain growth, and results in better crystallinity. FTIR and XRD studies of aluminas obtained from an aluminium waste showed similar results to those of aluminas obtained from conventional pure raw materials.

Aknowledgments The authors thank the company Recuperaciones y Reciclajes Roman S.L. (Fuenlabrada, Madrid, Spain) for supplying the waste and CSIC for the financial support.

Table 1 TG and DTA analysis of the precursor boehmite

| Effect | DTA | | | TG | |
|-------------------------|------------------------|-----------------------|---|------------------------|------------------|
| | Temperature range (°C) | Peak Temperature (°C) | Peak Integration ($\mu\text{V}\cdot\text{s}/\text{mg}$) | Temperature range (°C) | Mass Loss (wt %) |
| 1 endo | 64 - 246 | 123 | 64.1 | 50 - 244 | 12.7 |
| 2 endo | 296 - 485 | 404 | 44.7 | 244 - 500 | 15.1 |
| 3 not well-defined zone | --- | --- | --- | 500 - 1028 | 2.6 |
| 4 exo | 1062 - 1204 | 1152 | 16.6 | 1028 - 1400 | 0 |

Table 2 Composition of the calcined precursor at 1300 and 1400 °C for 7 h, obtained by FRX, (expressed as oxide wt. %)

| Compounds (wt %) | Calcination Temperature (°C) | |
|--------------------------------|------------------------------|--------------|
| | 1300 | 1400 |
| Al ₂ O ₃ | 94.11 | 94.91 |
| Fe ₂ O ₃ | 3.47 | 3.31 |
| SiO ₂ | 1.03 | 0.94 |
| ZnO | 0.54 | 0.44 |
| PbO | 0.20 | 0.14 |
| CuO | 0.17 | 0.09 |
| Cr ₂ O ₃ | 0.11 | 0.07 |

Table 3 Wavenumbers (cm^{-1}) of FTIR bands of the precursor boehmite together with the values and assignment from Refs. [3,17,21]

| Boehmite bands position (cm^{-1}) | | | | Assignment |
|---|-----------------------|----------------------|-------------------|--|
| This work | Ref. [17] | Ref. [21] | Ref. [3] | |
| 329 sh 364 - | - - - | 320 365 - | 326 368 405 | Deformation and Stretching mode AlO_6 and AlO_4 |
| 496 - 566 | - - 566 sh | 475 sh 525 600 | 491 - - | Deformation of angle OH-Al=O (ν_6) |
| 634 666 sh | 633 - | - | 616 | Bending in the plane of angle OH-Al=O (ν_5) |
| - - 880 | 740 sh - 885 sh | - 760 840 sh | 740 761 880 | O=A-O-H angle bending and Al=O bending (ν_4) |
| 1071 | 1068 | 980 1025 1075 | 1072 | Al=O stretching (ν_2) |
| 1155 sh | 1165 sh | 1150 sh | 1160 | O-H bending (ν_3) |

Figure Captions

Fig. 1 XRD patterns of the aluminium waste (1: Al, 2: Al₂O₃, 3: SiO₂, 4: AlN, 5: CaCO₃, 6: MgAl₂O₄)

Fig.2 XRD patterns of the precursor obtained by hydrothermal treatment of the aluminium waste.

(Indexation hkl according to JCPDS 1-088-2112 file)

Fig. 3 Field Emission Scanning electron micrograph of the precursor boehmite obtained by hydrothermal treatment of the aluminium waste.

Fig. 4 XRD patterns of calcined precursor at 1300 °C (a) and 1400 °C (b) for 7 h. (Indexation hkl according to JCPDS- 1-089-7717 file)

Fig. 5 Transmission electron microscopy of the precursor boehmite calcined at 1300 °C. In the upper left and right corners the electron diffraction images of the marked zones.

Fig. 6 Transmission electron microscopy of the precursor boehmite calcined at 1400 °C. a) Image of an aggregate with the corresponding electron diffraction. b) High resolution TEM image of the marked zone.

Fig. 7 FTIR spectra of boehmite and calcined samples at 1300 and 1400 °C.

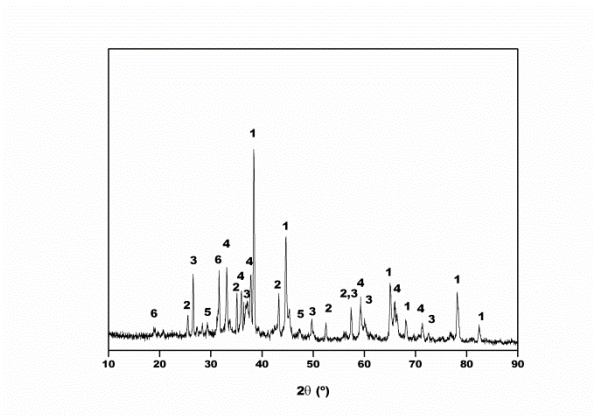


Fig. 1

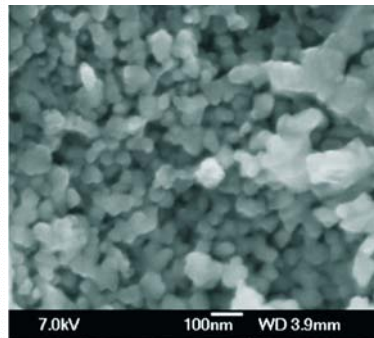


Fig.3

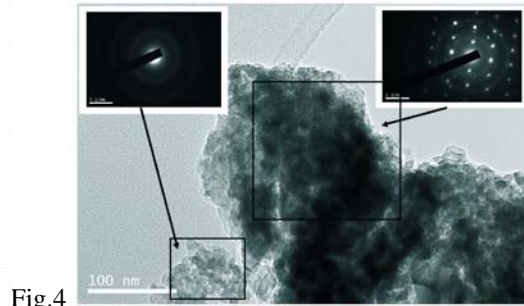
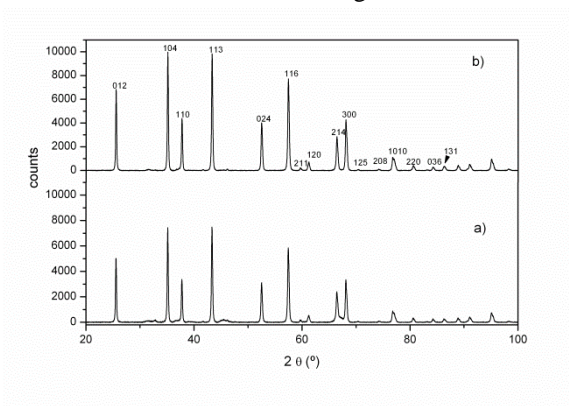


Fig.4

Fig.5

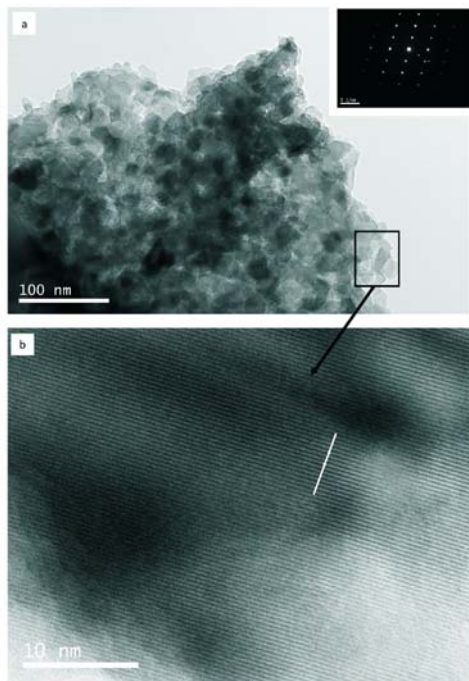


Fig.6

References

1. Sanchez-Valente J, Bokhimi X, Toledo JA (2004) Synthesis and catalytic properties of nanostructured aluminas obtained by sol-gel method. *Applied Catalysis a-General* 264 (2):175-181. doi:10.1016/j.apcata.2003.12.041
2. Souza-Santos. P.; Souza-Santos. H TSP (2000) Standard Transition Aluminas. *Electron Microscopy Studies. Materials Research* 3 (4):11. doi:10.1590/S1516-14392000000400003
3. Boumaza A, Favaro L, Ledion J, Sattonnay G, Brubach JB, Berthet P, Huntz AM, Roy P, Tetot R (2009) Transition alumina phases induced by heat treatment of boehmite: An X-ray diffraction and infrared spectroscopy study. *Journal of Solid State Chemistry* 182 (5):1171-1176. doi:10.1016/j.jssc.2009.02.006
4. Murali KR, Thirumoorthy P (2010) Characteristics of sol-gel deposited alumina films. *Journal of Alloys and Compounds* 500 (1):93-95. doi:10.1016/j.jallcom.2010.03.219
5. Li JS, Wang XY, Wang LJ, Hao YX, Huang YL, Zhang Y, Sun XY, Liu XD (2006) Preparation of alumina membrane from aluminium chloride. *Journal of Membrane Science* 275 (1-2):6-11. doi:10.1016/j.memsci.2005.08.011
6. Parida KM, Pradhan AC, Das J, Sahu N (2009) Synthesis and characterization of nano-sized porous gamma-alumina by control precipitation method. *Materials Chemistry and Physics* 113 (1):244-248. doi:10.1016/j.matchemphys.2008.07.076
7. Kim SM, Lee YJ, Jun KW, Park JY, Potdar HS (2007) Synthesis of thermo-stable high surface area alumina powder from sol-gel derived boehmite. *Materials Chemistry and Physics* 104 (1):56-61. doi:10.1016/j.matchemphys.2007.02.044
8. Wang YH, Wang J, Shen MQ, Wang WL (2009) Synthesis and properties of thermostable gamma-alumina prepared by hydrolysis of phosphide aluminum. *Journal of Alloys and Compounds* 467 (1-2):405-412. doi:10.1016/j.jallcom.2007.12.007
9. Wang XH, Lu GZ, Guo Y, Wang YS, Guo YL (2005) Preparation of high thermal-stable alumina by reverse microemulsion method. *Materials Chemistry and Physics* 90 (2-3):225-229. doi:10.1016/j.matchemphys.2004.11.012
10. Passos A, Martins L, Pulcinelli S, Santilli C Design of hierarchical porous aluminas by using one-pot synthesis and different calcination temperatures. *Journal of Sol-Gel Science and Technology*:1-9. doi:10.1007/s10971-011-2674-6
11. Schinkel G, Garrn I, Frank B, Gernert U, Schubert H, Schomacker R (2008) Fabrication of alumina ceramics from powders made by sol-gel type hydrolysis in microemulsions. *Materials Chemistry and Physics* 111 (2-3):570-577. doi:10.1016/j.matchemphys.2008.05.032
12. Gocmez H, Ozcan O (2008) Low temperature synthesis of nanocrystalline alpha-Al₂O₃ by a tartaric acid gel method. *Materials Science and Engineering a-Structural Materials Properties Microstructure and Processing* 475 (1-2):20-22. doi:10.1016/j.msea.2006.12.147
13. Martin MI, Rabanal ME, Gomez LS, Torralba JM, Milosevic O (2008) Microstructural and morphological analysis of nanostructured alumina particles synthesized at low temperature via aerosol route. *Journal of the European Ceramic Society* 28 (13):2487-2494. doi:10.1016/j.jeurceramsoc.2008.03.019
14. Ibrahim DM, Abu-Ayana YM (2009) Preparation of nano alumina via resin synthesis. *Materials Chemistry and Physics* 113 (2-3):579-586. doi:10.1016/j.matchemphys.2008.07.113

15. Nakano H, Makino Y, Sano S (2008) Microstructure of alumina produced by millimeter-wave heating. *Journal of Alloys and Compounds* 457 (1-2):485-489. doi:10.1016/j.jallcom.2007.03.007
16. López-Delgado A, Tayibi H (2011) Can hazardous waste become a raw material? The case study of an aluminium residue: a review. *Waste Management & Research*. doi:10.1177/0734242x11422931
17. Gonzalo-Delgado L, López-Delgado A, López FA, Alguacil FJ, López-Andrés S (2011) Recycling of hazardous waste from tertiary aluminium industry in a value-added material. *Waste Management & Research* 29 (2):127-134. doi:10.1177/0734242x10378330
18. Rinaldi R, Schuchardt U (2005) On the paradox of transition metal-free alumina-catalyzed epoxidation with aqueous hydrogen peroxide. *Journal of Catalysis* 236 (2):335-345. doi:10.1016/j.jcat.2005.10.007
19. Alphonse P, Courty M (2005) Structure and thermal behavior of nanocrystalline boehmite. *Thermochimica Acta* 425 (1-2):75-89. doi:10.1016/j.tca.2004.06.009
20. Jayaraman V, Periaswami G, Kutty TRN (1998) Influence of the preparative conditions on the precursor phases formed during the synthesis of beta-alumina by the wet chemical gel to crystallite conversions. *Materials Chemistry and Physics* 52 (1):46-53. doi:10.1016/s0254-0584(98)80005-9
21. Ram S (2001) Infrared spectral study of molecular vibrations in amorphous, nanocrystalline and AlO(OH) center dot alpha H2O bulk crystals. *Infrared Physics & Technology* 42 (6):547-560. doi:10.1016/s1350-4495(01)00117-7